WELDING RESEARCH

SUPPLEMENT TO THE *WELDING JOURNAL*, MARCH 2006
Sponsored by the American Welding Society and the Welding Research Council

Design of Experiment Analysis and Weld Lobe Estimation for Aluminum Resistance Spot Welding

A systematic experimental study reveals how welding parameters and abnormal process conditions affect the quality of aluminum resistance spot welds

BY Y. CHO, W. LI, AND S. J. HU

ABSTRACT. The effects of various process conditions on weld quality were studied for aluminum resistance spot welding. Along with major welding process parameters including current, time, and electrode force, abnormal process conditions such as poor fitup, axial misalignment, and angular misalignment were also examined using a systematic design of experiment method. The combinations of two and three levels of these factors were tested in the experiment and the corresponding weld button diameters were evaluated with peel tests. As an experimental method to estimate the weld lobe and quality, the two-stage, sliding-level design of experiment was used to consider the linear and quadratic effects of the process parameters. Through the analysis, mathematical models were established, based on which the influences of the welding parameters on the weld lobes and weld size were discussed. The significance of the process abnormalities and the recommendations for better weld quality were also presented.

Introduction

As the demand for lightweight and highly fuel-efficient automobiles increases, joining of aluminum alloy has become an important issue in the automotive industry. Aluminum alloy offers high strength-to-weight ratio and excellent corrosion resistance. It is therefore considered a substantial weight-saving alternative to traditional mild steels for vehicle body structures. For several decades, the joining of mild steel body structures has been done using resistance spot welding (RSW). Unlike other methods such as mechanical fastening and riveting, the RSW process is fast, flexible, and easy to maintain. Moreover, it is a well-established process in the automotive industry. As a result, there is a strong preference to using RSW in joining aluminum sheet metal parts. However, a serious concern exists on the quality of aluminum spot welds due to the difference between the RSW of steel and aluminum (Ref. 1). Compared to steel, aluminum has higher electrical and thermal conductivities, a narrower range between the solidus and liquidus temperatures (about 30°C), and a lower melting temperature around 670°C (Ref. 2). Aluminum also forms nonconductive films on its surfaces when exposed to air. All these properties make the RSW process of aluminum harder to control. Consequently, detailed studies are needed on the quality variation of the aluminum RSW process to achieve consistency in high-volume production (Ref. 3).

Most of the previous research on aluminum RSW was concentrated on the effects of major process parameters such as electrode force, current, time, electrode type, and surface conditions (Refs. 4–7). Shear strength and weld button diameter were used as measures of the weld quality. Early work on RSW of high-strength aluminum alloys in the aerospace industry has shown that riveting performed better in terms of the fatigue strength (Ref. 8). Later, high-strength spot-welded aluminum structures have been demonstrated in the automotive industry (Ref. 9). Among various methods of analyzing the effects of welding parameters, the weldability lobe diagram is one of the most powerful techniques that can be used to illustrate the effects of welding current and time. Kaiser et al. (Ref. 10), and Han et al. (Ref. 11), employed the lobe diagram to investigate the acceptable welding current and time for high-strength steel. The weld lobe diagram was also used to examine the coating effects of various types of coated steels, e.g., hot-dipped galvanized steel, electrogalvanized steel, and galvannealed steel (Refs. 12–14). Weld lobe diagrams are usually developed in a lab environment with nominal process settings and then extended to production. In a production environment, however, there are many abnormal process conditions that may result in large weld quality variation. The effects of the abnormal process conditions have been discussed by a number of researchers. Nagel and Lee considered abnormal conditions in order to develop a new automatic process control approach (Ref. 15). Karagoulis studied the effect of electrode misalignment in a plant environment and reported that a shift of the weldability lobe curves was observed because of the electrode misalignment (Ref. 16). Li, et al. conducted a systematic study on the effects of both normal and abnor-

KEYWORDS

Aluminum Alloy
Resistance Spot Welding
Two-stage, Sliding-level
Design of Experiment
Regression Analysis
Weld Lobe
Quality Estimation
Weld Quality

Y. CHO and S. J. HU are with Department of Mechanical Engineering, The University of Michigan, Ann Arbor, Mich. W. LI is with Department of Mechanical Engineering, University of Washington, Seattle, Wash.

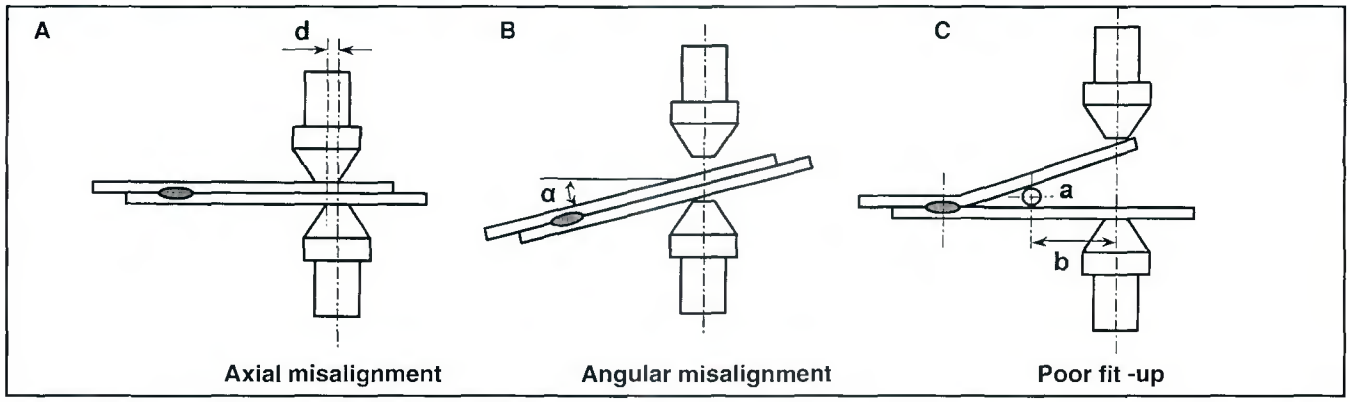

Fig. 1 — Abnormal process conditions in aluminum resistance spot welding.

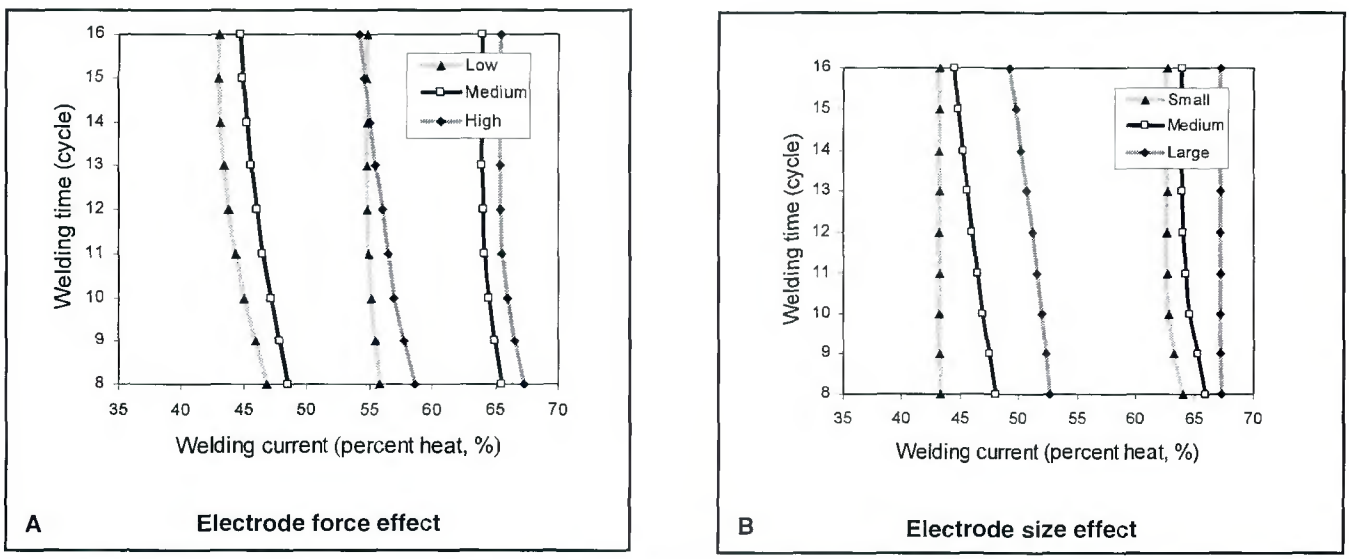

Fig. 2 — Effect of the major welding parameters on the weld lobes. A — Electrode force effect; B — electrode size effect.

Table 1 — Design Factors of the Experiment

Design Factors	Low	Medium	High
Current *I* (A)	Determined accordingly (sliding level)		
Time *T* (cycle)	8	12	16
Electrode force *F* (kN)	5.1	6.3	7.5
Electrode size *S* (mm)	25	50	75
Poor fitup *Fit* (mm)	0	—	5
Axial misalignment *Ax* (mm)	0	—	1.5
Angular misalignment *Ang* (°)	0	—	10

mal welding conditions (Ref. 17). Mathematical models were developed for process analysis and improvement. All the above research, however, was focused on the RSW of mild steels. A systematic study on the effects of various process conditions for the aluminum RSW process has not been reported.

In this study, the effects of various welding conditions on the quality of aluminum welds were investigated using the design of experiment and statistical modeling approach. Both process parameters and abnormalities, such as electrode misalignment and poor fitup, were examined. Because of the complexity of the combinations and the interdependency among the process parameters, a newly developed two-stage, sliding-level experiment (Ref. 17) was used for the experimental design and analysis. Mathematical models were developed for estimating the weld size and weldability lobe curves, both of which were used as response variables to analyze the effects of the process conditions. The proprieties of the models and recommendations for better weld quality were also presented.

Experimental Procedure

The experiments were performed using 2.0-mm commercial aluminum Alloy AA5754 on a mid-frequency DC welding machine. The electrodes were dome-type with a spherical surface. Welding parameters, such as welding current, time, and electrode force, were examined with a number of abnormal process conditions. The abnormal conditions considered in this study were recommended by a group of experienced welding engineers. These conditions included axial misalignment, angular misalignment, and poor fitup, as shown in Fig. 1. Axial misalignment *Ax* in Fig. 1A indicates that the axes of the upper and lower electrodes deviate

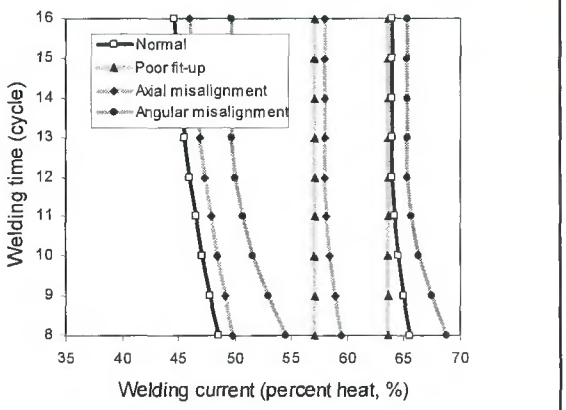

A **Medium electrode force with medium electrode size**

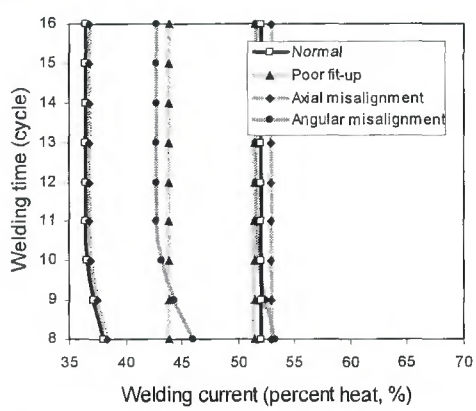

B **Low electrode force with small electrode size**

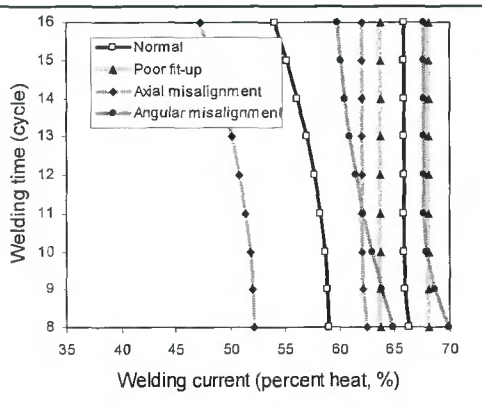

C **High electrode force with large electrode size**

Fig. 3 — Examples of effects of the abnormal conditions on the weld lobes. A — Medium electrode force with medium electrode size; B — low electrode force with small electrode size; C — high electrode force with large electrode size.

from each other by a distance *d*. Figure 1B shows the angular misalignment condition *Ang* in which the parts are tilted relative to the axis of the electrode by an angle of α. When the two sheet metal parts separate, a poor fitup condition *Fit* exists. This condition was created by inserting a piece of wire with a diameter of *a* at a distance *b* from the centerline of the electrodes, as shown in Fig. 1C. A specially designed fixture was used to produce the above abnormal conditions.

In the design of experiment, the factors considered were the abnormal process conditions and the major welding parameters, including welding current *I*, time *T*, and electrode force *F*. In case of electrode wear, electrode size *S* (spherical radius) was used since it was assumed that the electrode wear affected the process through the change of the electrode face diameter. The settings of these factors in the experiment were determined based on previous process knowledge. Two levels were used for the abnormal process conditions and three levels for the major welding parameters and electrode size. The settings of the factors in the experiment are listed in Table 1.

In order to study the effects of the abnormal process conditions with various welding parameters, the two-stage, sliding-level method was employed in the design and analysis of the experiment. This method was necessary because of the interdependency among the variables in the resistance spot welding process. Specifically, there is an acceptable range for the welding current as shown in a typical weld lobe diagram. As such, the experiment had to be conducted in two stages. The first stage was used to determine the suitable current range under each designed experimental condition; and the second stage was used to perform test welds on the settings determined at the first stage.

The experiment matrix is shown in Table 2. The first three columns are for the three-level factors. The levels are low, medium, and high, represented by 1, 2, and 3, respectively. The last three columns are for the two-level factors whose levels are described as –1 and 1, with –1 indicating the low level and +1 indicating the high level. For each of these settings, a current range was determined based on a standard weld lobe development procedure (Ref. 18). After the current ranges were found, the experiment was carried out based on the results from the first stage to evaluate the weld quality. The welded samples were peeled and the diameters of the weld buttons measured following a standard weld quality evaluation procedure (Ref. 19).

Response Modeling

A statistical regression analysis was performed to analyze the quality of aluminum resistance spot welds in terms of the weld lobe and weld diameter. The relationships among the acceptable current range, weld diameter, and the welding parameters were characterized using mathematical models. The response variables of the models were different at different stages of the experiment. At the first stage, the current range was selected as the response variable. In order to facilitate the analysis, the current range of the weld lobe was converted into two independent response variables, the center of the current range I_C and the length of the current range I_L. At the second stage, the response variable was the weld button size.

In this study, two groups of factors were used to construct the response models through a regression analysis. One group was the two-level factors such as poor fitup, axial misalignment, and angular misalignment. The other group was the three-level factors consisting of electrode force, welding time, and electrode size. In the regression analysis, the first group of variables contributed to the first-order regressors. The second group contributed to both the first- and second-order regressors. In addition, the interactions among the independent regressors were also included in the response models. In order to avoid inaccurate estimation due to co-linearity among the above terms, an orthogonal coding system was introduced. For the three-level variables, the physical values were normalized to [–1 0 –1] for the first-order linear effect x_1 and to [1 –2 1] for the second-order qua-

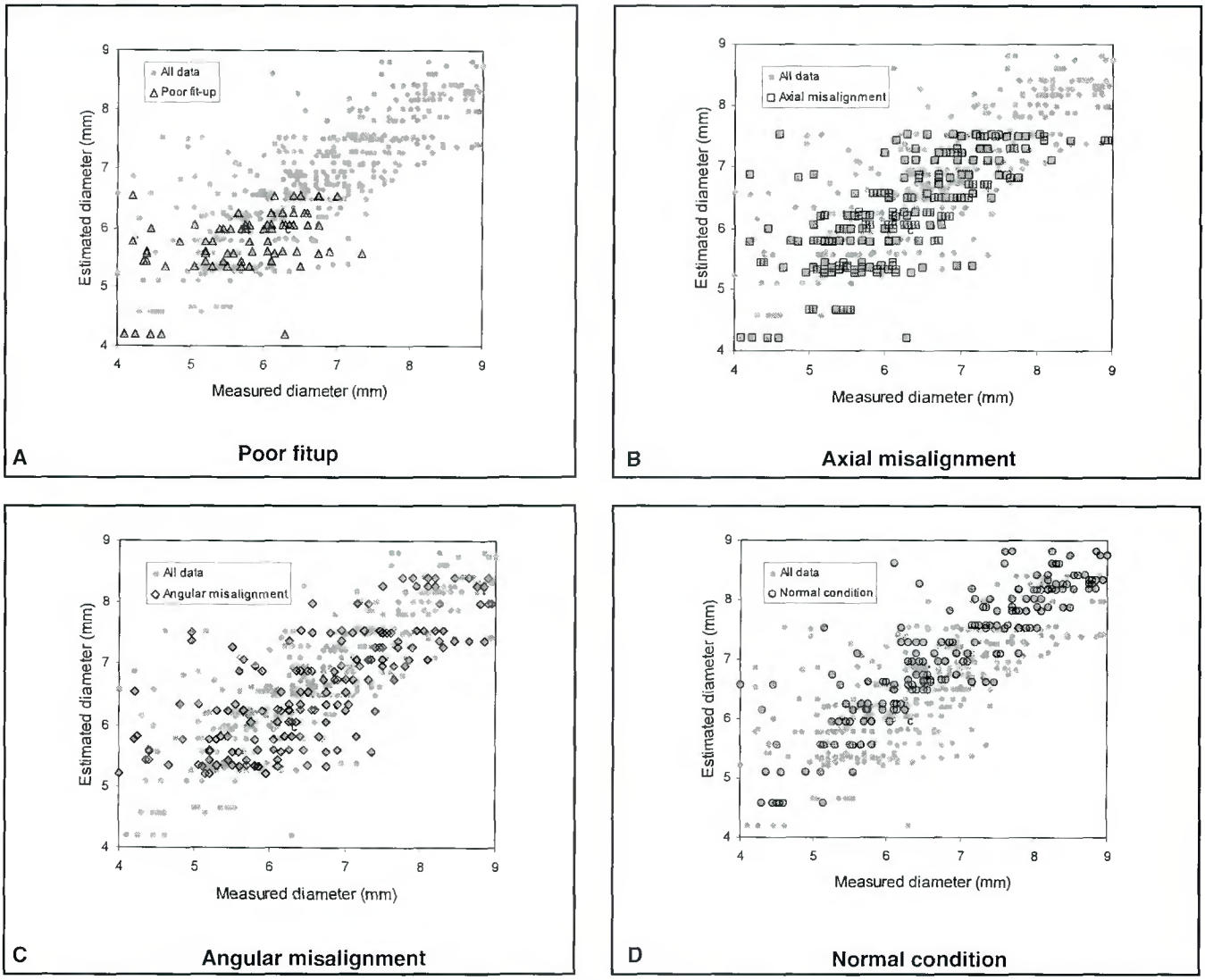

Fig. 4 — Relationship between measured and estimated weld diameter. A — Poor fitup; B — axial misalignment; C — angular misalignment; D — normal condition.

dratic effect x_2. The normalizations are defined in the following equations.

$$x_1 \begin{cases} \dfrac{x - x_l}{x_m - x_l} - 1, & x_l \le x \le x_m \\ \dfrac{x - x_m}{x_n - x_m}, & x_m \le x \le x_n \end{cases} = \begin{cases} -1, & x = x_l \\ 0, & x = x_m \\ 1, & x = x_n \end{cases} \quad (1)$$

$$x_2 = \vec{x} \cdot \left(\vec{X}^T \cdot \vec{X} \right)^{-1} \cdot \vec{X}^T \cdot \vec{Y} = \begin{cases} 1, & x = x\ell \\ -2, & x = x_m \\ 1, & x = x_n \end{cases} \quad (2)$$

where x_l, x_m, and x_n are the settings for low, medium, and high values of the factors, respectively. Due to the difference of response variables in the two stages of the experiment, current range and weld size were analyzed separately during the regression analysis.

Current Range Analysis

Before performing the regression analysis, the correlation coefficients between the dependent variables including the center and the length of the current range and the independent variables including the linear and quadratic effects of electrode size, force, and welding time and the linear effects of poor fitup, axial misalignment, and angular misalignment were calculated and listed in Table 3. Subscript 1 stands for the linear effect. Subscript 2 stands for the quadratic effect. From the table, it can be seen that electrode force, followed by electrode size, is the most dominant factor affecting the center of the current range. The abnormal conditions themselves do not play an important role on the center of the current range. However, they have strong influences on the length of the current range, e.g., the poor fitup condition *Fit* has a correlation coefficient of –0.840 with I_L. In general, the second-order quadratic effects have lower correlation than the first-order linear effects. Nonetheless, they significantly affect the center and length of the current range when their interactions with other factors are considered. This can be seen in Equations 3 and 4, where the interaction terms such as T_2**Fit* and F_2**Ax* are included in the response models.

Usually, the larger the correlation coefficient is, the larger the effect a variable will have. However, because the correlation coefficient depends only on the linear relationship between the response and the

variable, a more advanced regressor selection procedure is required. To develop more reliable models, a stepwise regression method (Refs. 20, 21) was applied in this study. The regressors were selected from the independent variables including the linear, quadratic effects of the variables and the interactions among them. The independent variables were entered into the regression model one by one depending on their probabilistic significance to the response variable. The obtained models are as follows:

$$I_C = 57.39 + 4.17*F_1 - 3*T_1*S_1 + 2.5*S_1 - 2*Fit*Ang - 1.167*Ax - 1.5*F_1*Ax - 0.92*T_1*S_1 - 0.67*T_2*Fit + 0.5*S_2 + 0.33*T_2*Ang + 0.583*T_1*S_2 - 0.25*T_2*S_1 + 0.03*T_2*S_2 \quad (3)$$

$$I_L = 8.139 - 4.417*Fit + 2.0*Ax*Ang + 1.833*F2*Ax - 1.000*T1*Fit - 0.833*Ang + 1.167*F1*T2 + 0.667*S_1*Ang + 1.667*T_1*S_1 + 0.139*T_2 - 0.500*\mathrm{Fit}*\mathrm{Ax} - 0.667*\mathrm{S}_1 - 0.250*T_2*\mathrm{Fit} - 0.111*\mathrm{S}_2 - 0.167*T_1*Ang \quad (4)$$

The standardized regression coefficients are listed in Tables 4 and 5. These coefficients can be used to interpret the significance of individual regressors. As can be seen from these tables, the linear effects of electrode force F_1 and electrode size S_1 have the most significant influence on the center of the current range I_C. The interaction between welding time and electrode size T_1*S_1 and that between poor fitup and angular misalignment $Fit*Ang$ also play an important role. In case of the length of the current range I_L, poor fitup *Fit* shows the strongest influence, followed by the interactions between the quadratic effect of electrode force and axial misalignment F_2*Ax and that between axial misalignment and angular misalignment $Ax*Ang$.

Weld Button Size Analysis

A similar procedure was also performed to develop an estimation model for the weld button size. In addition to the factors for the current range analysis, two new variables, the linear and quadratic effects (I_1 and I_2) of the given welding current, and their interactions with other variables were added to the button size analysis. Equation 5 shows the result of the analysis. The coefficient of determination R^2 is 0.944 and the standard error of the estimation is 0.3014. Therefore, more than 94.4% of the button size variance can be explained by the model.

$$\mathrm{Dia} = 6.214 - 0.477*Fit + 0.665*I_1 + 0.554*F_1 - 0.42*Fit*I_1 - 0.317*S_1*Fit - 0.241*Ax - 0.439*\mathrm{S}_1*Ax - 0.185*T_2 + 0.276*\mathrm{F}_1*Ang - 0.082*I_2 + 0.071*Fit*\mathrm{I}_2 + 0.0963*Ax*Ang \quad (5)$$

Standardized regression coefficients in Table 6 show that poor fitup *Fit*, the linear effect of welding current I_1, the linear effect of electrode force F_1, the interaction effect between poor fitup and welding current $Fit*I_1$, and the interaction effect between electrode size and axial misalignment S_1*Ax are the dominant factors in the button size estimation model.

Table 2 — Experiment Matrix

	Electrode Force (*F*)	Time (*T*)	Electrode Size (*S*)	Poor fitup (*Fit*)	Axial Misalignment (*Ax*)	Angular Misalignment (*Ang*)
1	1	1	1	-1	-1	-1
2	1	1	2	-1	1	-1
3	1	1	3	-1	-1	1
4	1	2	3	1	-1	1
5	1	3	1	1	1	1
6	1	3	3	1	1	-1
7	2	1	1	1	1	-1
8	2	1	2	1	1	1
9	2	2	1	-1	-1	1
10	2	2	2	-1	-1	-1
11	2	2	3	-1	1	-1
12	2	3	1	1	-1	1
13	3	1	2	1	-1	1
14	3	2	2	1	1	-1
15	3	2	3	1	1	1
16	3	3	1	-1	1	-1
17	3	3	2	-1	-1	1
18	3	3	3	-1	-1	-1

Table 3 — Correlation Coefficients of Welding Current and Independent Variables

	F_1	F_2	T_1	T_2	S_1	S_2	Fit	Ax	Ang
I_C	0.594	0.234	0.297	-0.093	0.513	-0.187	-0.022	-0.176	0.132
I_L	0.164	0.013	0.140	-0.027	-0.164	-0.067	-0.840	-0.305	-0.458

Results and Discussion

Using the response models described in Equations 3–5, the effects of various welding parameters can be discussed based on the predictions of the weld lobes and the weld button diameters. Figure 2 shows the effects of electrode force and size on the weld lobe under normal and medium electrode size or force conditions. In Fig. 2A, the black lines with rectangular marks show the lobe curves when the medium electrode force level (6.3 kN) is used. It is seen that acceptable welds can be made in a range between 48% and 65% of heat when the welding time is 8 cycles. Percentage heat is a measure of the welding current. In this case, 50% heat is corresponding to 21.2 kA. When the electrode force becomes lower or higher, the current ranges both become narrower. In case of the low electrode force of 5.1 kN (shown in light-gray lines with triangles), the upper boundary of the lobe shifts to the left, indicating early expulsions caused by insufficient electrode force. The lower boundary also shifts slightly to the left, showing an early nugget formation due to the high initial contact resistance caused by the low electrode force. When the high electrode force of 7.5 kN is used, a different type of change of the lobe curves is observed as shown in the dark-gray lines with diamonds in the figure. The lower boundary is moved to the right, which indicates that excessive electrode force can cause the initial contact resistance to decrease due to the early collapse of asperities on the contact surfaces. The decreased contact resistance requires a higher welding current to produce enough heat in order to form a nugget. However, it is interesting to see that the upper boundary of the lobe does not shift to the right as much. This implies that using a higher electrode force does not help increase the expulsion limit.

The effects of electrode size are shown in Fig. 2B. The lobe curve shifts are also

Table 4 — Standardized Regression Coefficients for I_C

F_1	T_1*S_1	S_1	Fit*Ang	Ax	F_1*Ax	T_1*S_1	T_2*Fit	S_2	T_2*Ang	T_1*S_2	T_2*S_1	T_2*S_2
0.674	-0.396	0.405	-0.374	-0.231	-0.243	-0.121	-0.187	0.140	0.093	0.128	-0.055	0.011

Table 5 — Standardized Regression Coefficients for I_L

Fit	Ax*Ang	F_2*Ax	T_1*Fit	Ang	F_1*T_2	S_1*Ang	T_1*S_1	T_2	Fit*Ax	S_1	T_2*Fit	S_2	T_1*Ang
-0.759	0.324	0.445	-0.140	-0.143	0.214	0.094	0.191	0.034	-0.081	-0.094	-0.061	-0.027	-0.023

Table 6 — Standardized Regression Coefficients for Weld Button Diameter

Fit	I_1	F_1	Fit*I_1	S_1*Ax	Ax	S_1*Fit	T_2	F_1*Ang	I_2	Fit*I_2	Ax*Ang
-0.430	0.489	0.407	-0.306	-0.323	-0.217	-0.234	-0.235	0.203	-0.104	0.090	0.082

Table 7 — Estimation Results in Terms of Correlation Coefficients and Standard Errors

	Poor fitup		Axial misalignment		Angular misalignment		Normal condition	
	R	Er	R	Er	R	Er	R	Er
All data	0.552	0.499	0.731	0.581	0.774	0.605	0.870	0.555

observed when the electrode size varies. When smaller electrodes are used, the weld lobe shifts to the left (light-gray lines with triangles), showing that less current is needed to produce an acceptable weld. This is because the current density through the faying surface increases as the electrode size decreases. On the other hand, as larger electrodes are used (dark-gray lines with diamonds), more current is required to produce an acceptable weld. In this case, the upper boundary does not shift as much as the lower one. This means that an excessive electrode size can cause unwanted decrease in the length of the current range. Although the small electrode size yields a slightly wider weld lobe, the current density will be much higher when using smaller electrodes to make the same sized welds. Using small electrodes could accelerate the electrode wear, which should always be avoided in production.

Figure 3 shows the effects of the three abnormal process conditions on the weld lobes. The effects of the abnormal conditions at the medium electrode force and size are shown in Fig. 3A. As can be seen, the widest acceptable current range is obtained under the normal condition (black lines with rectangles). In the case of poor fitup condition (light-gray lines with triangles), the lower boundary of the weld lobe shifts to the right dramatically, while the upper boundary remains more or less the same as the normal condition. This has resulted in a much narrower current range and thus a less robust welding process. When axial misalignment exists (mid-gray lines with diamonds), expulsions occur with less heat input. However, there is no significant difference in the minimum heat to obtain an acceptable weld. Angular misalignment causes a slight shift of the lower boundary toward the right (dark-gray lines with circles), indicating an increase in the minimum current requirement. However, the upper boundary also increases slightly. Figure 3B shows the effects of abnormal conditions at low electrode force and small electrode size. In general, the acceptable current ranges tend to move toward the low current side comparing to the case for medium electrode force and size. Especially, the upper boundaries are around 50–55% of heat, suggesting that the current required to produce an acceptable weld is much smaller. Poor fitup and angular misalignment makes the current ranges narrower. There is almost no effect by the axial misalignment. The case for high electrode force and large electrode size is shown in Fig. 3C. Overall, the lobe curves move toward the high current side and the acceptable current ranges become narrower, too. Compared to the other abnormal conditions, the axial misalignment requires less current to form an acceptable weld. This is because axial misalignment reduces the effective contact area for current flow at the faying surface, which in turn results in increased current density and earlier nugget formation.

The effects of the abnormal conditions on the weld diameter are shown in Fig. 4. The estimated weld diameters are plotted against the measured ones for all the abnormal and normal process conditions. In these plots, each experimental data point including its replicates is represented with a gray dot. The data points corresponding to individual abnormal and normal conditions are indicated using special marks, triangles for poor fitup in Fig. 4A, squares for axial misalignment in Fig. 4B, diamonds for angular misalignment in Fig. 4C, and circles for the normal condition in Fig. 4D. By representing the experimental data this way, the effects of abnormal conditions can be visualized clearly with respect to the overall data set.

Figure 4A shows the effect of the poor fitup condition. Comparing to the measured weld diameters across all the conditions, poor fitup gives rise to smaller weld nuggets. This may mean that the poor fitup condition has the strongest detrimental effect on the weld size. The correlation between the estimated and measured weld diameters does not follow a good linear trend, which indicates that the statistical model does not predict the weld diameter well under the poor fitup condition. Figure 4B shows the effect of axial misalignment. It is seen that large weld diameters up to 8–9 mm can still be made under this abnormal process condition. The correlation between the measured and estimated weld diameters is reasonably strong. Similarly, large welds can also be made under the angular misalignment

condition and the statistical model predicts the weld diameter fairly well, as shown in Fig. 4C. Figure 4D shows the weld diameters under the normal condition. The correlation between the measured and estimated seems to be the best among all the process conditions. This result is expected since the variation caused by the abnormal conditions is excluded.

The correlations between the estimated and measured weld diameters and the estimated errors for each of the process conditions are presented in Table 7. The correlation coefficient is represented as *R* and standard error of the estimation as *Er*. The correlation coefficients agree with the observations from Fig. 4, with the lowest for the poor fitup condition (0.552) and the highest for the normal condition (0.870). The standard errors are comparable among all the cases, which is about 0.5–0.6 mm.

Conclusions

The effects of various welding parameters in aluminum resistance spot welding were investigated using a systematic two-stage, sliding-level design of experiment approach. The following conclusions are obtained from this study:

1) From the statistical models, it is shown that the linear effects of electrode force and size have the most significant influence on the center of the current range. The poor fitup condition and the interaction between the quadratic effect of electrode force and axial misalignment have significant effects on the length of the current range.

2) When a medium electrode force is applied, the acceptable current range is the widest. Both lower and higher electrode force will reduce the length of the current range, which means a less robust welding process.

3) Among the abnormal process conditions, the poor fitup condition has the strongest detrimental effect on the quality of aluminum resistance spot welding. It causes small weld diameters and thus weak joints. In addition, the effect of poor fitup is hard to characterize using a statistical model.

4) In general, abnormal process conditions cause narrower weld lobes. In order to minimize the effects of these abnormalities, more heat input is recommended within the limits of acceptable current ranges to avoid expulsion.

Acknowledgments

This work was supported by NIST/ATP Intelligent Resistance Welding through Auto Body Consortium. Support for Cho's postdoctoral fellowship program from the Korea Science and Engineering Foundation (KOSEF) is also gratefully acknowledged.

References

1. Senkara, J.. and Zhang, H. 2000. Cracking in spot welding aluminum alloy AA5754. *Welding Journal* 79(7): 194-s to 201-s.

2. Urech, W., and Gordon, H. F. 1986. Aluminum projection welding in industrial-scale production. *AWS Sheet Metal Conference II*, Paper No. 17.

3. Newton, C. J., Browne, D. J., Thornton, M. C., Boober, D. R., and Keay, B. F. P. 1994. The fundamentals of resistance spot welding aluminum, *Sheet Metal Conference VI*, Paper E2.

4. Hoglund, G. O., and Bernard, G. S., Jr. 1938. The effect of current, pressure and time on the shear strength and structure of spot welds in the aluminum alloys. *Welding Journal* 17(11): 45-s to 54-s.

5. Keller, F., and Smith, D. W. 1944. Correlation of the strength and structure of spot welds in aluminum alloys. *Welding Journal* 23(1): 23-s to 26-s.

6. Roset, C. A., and Rager, D. D. 1974. Resistance welding parameter profile for spot welding aluminum. *Welding Journal* 53(12): 529-s to 536-s.

7. Rönnhult, T., Rilby, U., and Olefjrd, I. 1980. The surface state and weldability of aluminum alloys. *Mat. Sci. Eng.* 42: 329 – 336.

8. Welter, O., and Croquet, A. 1954. Stress distribution and fatigue resistance of ALCLAD 24ST multiple spot welds. *Welding Journal* 33(2): 91-s to 98-s.

9. Thornton, P. H., Krause, A. R., and Davies, R. G. 1996. The aluminum spot weld. *Welding Journal* 75(3): 101-s to 108-s.

10. Kaiser, J. G., Dunn, G. J., and Eagar, T. W. 1982. The effect of electrical resistance on nugget formation during spot welding. *Welding Journal* 61(6):167-s to174-s.

11. Han, A., Indacochea, J. E., Chen, C. H., and Bhat, S. 1993. Weld nugget development and integrity in resistance spot welding of high-strength cold-rolled sheet steels. *Welding Journal* 72(5): 209-s to 265-s.

12. Gould, J. E., and Peterson, W. A. 1989. A detailed examination of weldability lobes for a range of zinc-coated steels, *SAE Technical Paper No. 880279.*

13. Howe, P., and Kelley, S. C. 1989. A comparison of the resistance spot weldability of bare, hot-dipped, galvannealed, and electrogalvanized DQSK sheet steels, *SAE Technical Paper No. 880280.*

14. Bowers, R. J., Sorensen, C. D., and Eagar, T. W. 1990. Electrode geometry in resistance spot welding. *Welding Journal* 69(2): 45-s to 51-s.

15. Nagel, G. L., and Lee, A. 1988. A new approach to spot welding feedback control. *SAE Technical Paper No. 880371.*

16. Karagoulis, M. 1992. Control of materials processing variables in production resistance spot welding. *Proc. AWS Sheet Metal Welding Conference V*, Detroit, Mich., Paper No. B5.

17. Li, W., Cheng, S., Hu, S., and Shriver, J. 2001. Statistical investigation of resistance spot welding quality using a two-state, sliding-level experiment. *ASME Journal of Manufacturing Science and Engineering*, 123: 523–520.

18. General Motors Corp. 1985. *Specifications and Procedures for Determining the Weldability of Body Steel Materials.*

19. Auto/Steel Partnership (A/SP). 1995. *Weld Quality Test Method Manual*, Standardized Test Method Task Force.

20. Montgomery, D. C. 2001. *Design and Analysis of Experiments*, 5th edition, John Wiley.

21. Hamada, M., and Wu, C. F. J. 1992. Analysis of designed experiments with complex aliasing. *Journal of Quality Technology* 24(3): 130–137.

Dear Readers:

The *Welding Journal* encourages an exchange of ideas through letters to the editor. Please send your letters to the Welding Journal Dept., 550 NW LeJeune Rd., Miami, FL 33126. You can also reach us by FAX at (305) 443-7404 or by sending an e-mail to Kristin Campbell at *kcampbell@aws.org.*